SINGLE-FEED DUAL BEAM SWITCHABLE ARRAY ANTENNA FOR ISM BAND APPLICATION

By

Naznin Akther

19METE016P

A thesis submitted in partial fulfilment of the requirements for the degree of MASTER of SCIENCE in Electronics and Telecommunication Engineering

Department of Electronics and Telecommunication Engineering

CHITTAGONG UNIVERSITY OF ENGINEERING AND TECHNOLOGY

MAY 2023

Declaration

I hereby declare that the work contained in this Thesis has not been previously submitted to meet requirements for an award at this or any other higher education institution. To the best of my knowledge and belief, the Thesis contains no material previously published or written by another person except where due reference is cited. Furthermore, the Thesis complies with PLAGIARISM and ACADEMIC INTEGRITY regulation of CUET.

Naznin Akther
19METE016P
Department of Electronics and Telecommunication Engineering
Chittagong University of Engineering & Technology (CUET)

List of Publications

Conference

- N. Akther, M. Hasan, M. A. Hossain, E. Nishiyama, I. Toyoda, "Experimental Study of a Single-Feed Dual-Beam Switchable Array Antenna Using PIN Diodes for 5.8-GHz Application", International Conference on Recent Progresses in Science, Engineering and Technology (ICRPSET), Rajshahi University, 26-27 December, 2022.

Journal

- M. Hasan, N. Akther, M. A. Hossain, E. Nishiyama, I. Toyoda, "A single-feed multi-beam pattern switchable array antenna using SPDT switches and hybrid couplers", Journal of Engineering. (Submitted)

Approval/Declaration by the Supervisor(s)

This is to certify that Naznin Akther has carried out this research work under my supervision, and that she has fulfilled the relevant Academic Ordinance of the Chittagong University of Engineering and Technology, so that she is qualified to submit the following Thesis in the application for the degree of MASTER of SCIENCE in Electronics and Telecommunication Engineering. Furthermore, the Thesis complies with the PLAGIARISM and ACADEMIC INTEGRITY regulation of CUET.

Dr. Md. Azad Hossain

Professor

Department of Electronics and Telecommunication Engineering

Chittagong University of Engineering & Technology

Acknowledgement

I am grateful to Almighty Allah for giving me good health and well-being. I wish to express my sincere gratitude to Dr. Md. Azad Hossain, supervisor of my thesis, Professor & Head of the Department of Electronics and Telecommunication Engineering, for providing me necessary facilities for the research. I would like to extend my appreciation to my mentor, Ichihiko Toyoda, Professor and Maodudul Hasan, Assistant Professor, Department of Electrical and Electronic Engineering, Saga University for their guidance through research collaboration.

In addition, I take this opportunity to express my gratitude to my parents, and family members for their continuous encouragement, and support throughout my life which motivated me to pursue post-graduation degree..

Abstract

This manuscript proposes one single-feed dual-beam switchable array antenna and one single-feed multi-beam switchable array antenna. The proposed antenna contains three and four microstrip square patch antenna elements and a switchable feed network respectively. In dual-beam design, the feed network creates a 90^0 phase difference between the center element and the right or left antenna elements. This antenna can tilt its main beam direction to $\theta = \pm 12°$ by exciting either right or left antenna elements along with the center patch through two PIN diodes, respectively. The dual-beam switching concept is experimentally verified with better than 8 dBi gain for every condition at $\phi = 0^0$-plane. The proposed multi-beam array antenna has two 90^0 switchable phase shifters. The 90^0 switchable phase shifter consists of a single-pole double-throw (SPDT) switch and a hybrid coupler. The hybrid coupler generates a 90^0 phase difference between the antenna elements to tilt its radiation pattern. The two SPDT switches can generate three modes to control the input ports of the hybrid coupler. As a result, two tilted beams and one difference pattern are generated from the same structure. A prototype multi-beam antenna is fabricated to demonstrate the concept experimentally. The measured results confirm the concept with a good agreement between the simulation and measurement. Better than 20dB cross-polarization suppression is achieved in the measurement.

বিমূর্ত

এই পাণ্ডুলিপিটি একটি একক-ফিড ডুয়াল-বিম স্যুইচযোগ্য অ্যারে অ্যান্টেনা এবং একটি একক-ফিড মাল্টি-বিম সুইচযোগ্য অ্যারে অ্যান্টেনার প্রস্তাব করে। প্রস্তাবিত অ্যান্টেনায় যথাক্রমে তিনটি এবং চারটি মাইক্রোস্ট্রিপ স্কয়ার প্যাচ অ্যান্টেনা উপাদান এবং একটি পরিবর্তনযোগ্য ফিড নেটওয়ার্ক রয়েছে। ডুয়াল-বিম ডিজাইনে, ফিড নেটওয়ার্ক কেন্দ্রের উপাদান এবং ডান বা বাম অ্যান্টেনা উপাদানগুলির মধ্যে একটি 90^0 ফেজ পার্থক্য তৈরি করে। এই অ্যান্টেনাটি যথাক্রমে দুটি পিন ডায়োডের মাধ্যমে কেন্দ্রের প্যাচের সাথে ডান বা বাম অ্যান্টেনা উপাদানগুলিকে উত্তেজনাপূর্ণ করে $\theta = \pm 12^\circ$ এর প্রধান রশ্মির দিকে কাত করতে পারে। ডুয়াল-বিম স্যুইচিং ধারণাটি পরীক্ষামূলকভাবে $\phi = 0^0$-প্লেনে প্রতিটি অবস্থার জন্য 8 dBi লাভের চেয়ে ভালো করে যাচাই করা হয়। প্রস্তাবিত মাল্টি-বিম অ্যারে অ্যান্টেনায় দুটি 90^0 টি পরিবর্তনযোগ্য ফেজ শিফটার রয়েছে। 90^0 পরিবর্তনযোগ্য ফেজ শিফটারে একটি একক-পোল ডাবল-থ্রো (SPDT) সুইচ এবং একটি হাইব্রিড কাপলার রয়েছে। হাইব্রিড কাপলার তার বিকিরণ প্যাটার্নকে কাত করতে অ্যান্টেনা উপাদানগুলির মধ্যে একটি 90^0 ফেজ পার্থক্য তৈরি করে। হাইব্রিড কাপলারের ইনপুট পোর্ট নিয়ন্ত্রণ করতে দুটি SPDT সুইচ তিনটি মোড তৈরি করতে পারে। ফলস্বরূপ, একই কাঠামো থেকে দুটি কাত বিম এবং একটি পার্থক্য প্যাটার্ন তৈরি হয়। ধারণাটি পরীক্ষামূলকভাবে প্রদর্শন করার জন্য একটি প্রোটোটাইপ মাল্টি-বিম অ্যান্টেনা তৈরি করা হয়েছে। পরিমাপ করা ফলাফল সিমুলেশন এবং পরিমাপের মধ্যে একটি ভাল চুক্তির সাথে ধারণাটিকে নিশ্চিত করে। পরিমাপে 20 dB ক্রস-পোলারাইজেশন দমনের চেয়ে ভাল।

Table of Contents

Abstract v
Table of Contents vii
List of Figures viii
List of Tables x
Chapter 1: INTRODUCTION 1
1.1 Background 1
1.2 Problem Statement 2
1.3 Aims and Objectives 2
1.4 Significance, Scope and Definitions 3
1.5 Thesis Outline 3
Chapter 2: LITERATURE REVIEW 4
Chapter 3: DUAL-BEAM SWITCHABLE ARRAY ANTENNA 9
3.1 Antenna Structure 9
3.2 Operating Principle 10
3.2.1 PIN Diode 10
3.2.2 Proposed Antenna 11
3.3 Design 14
3.4 Antenna Performance 15
Chapter 4: MULTI-BEAM SWITCHABLE ARRAY ANTENNA 19
4.1 Antenna Structure 19
4.2 Operating Principle 21
4.2.1 Hybrid Coupler 21
4.2.2 Proposed Antenna 23
4.3 Design 27
4.4 Antenna Performance 29
Chapter 5: CONCLUSION AND FUTURE WORKS. 36
Bibliography 37
Appendices ..... Error! Bookmark not defined.

List of Figures

Fig. No. **Figure Caption** **Page No.**

Figure 3.1-1: Structure design of the proposed 5.8-GHz single-feed dual-beam switchable array antenna 10

Figure 3.2-1: PIN Diode (i) symbol, (ii) structure 11

Figure 3.2-2: Fundamental theory of the proposed antenna 12

Figure 3.2-3: Simulated 3D radiation pattern of the proposed array antenna at 5.8-GHz, (i) D1 ON ($\phi = 0^0$). (ii) D1 ON ($\phi = 90^0$). (iii) D2 ON ($\phi = 0^0$). (iv) D2 ON ($\phi = 90^0$). 13

Figure 3.3-1: Optimized parameters of the proposed antenna.....14

Figure 3.4-1: Fabricated prototype of the presented 5.8-GHz dual-beam switchable single-feed antenna array. (i) Top view. (ii) Bottom view.....16

Figure 3.4-2: Measured and simulated reflection coefficient.....16

Figure 3.4-3: Measured and simulated radiation patterns for D1 ON condition. (i) $\phi = 0^0$-plane. (ii) $\phi = 90^0$-plane. 17

Figure 3.4-4: Measured and simulated radiation patterns for D2 ON condition. (i) $\phi = 0^0$-plane. (ii) $\phi = 90^0$-plane. 18

Figure 4.1-1: Block Diagram of the proposed three-state pattern reconfigurable antenna. 20

Figure 4.1-2: Schematic layout and cross-sectional view of the proposed 5.8-GHz multi-beam array antenna. 21

Figure 4.2-1: Structure of 90^0-hybrid coupler. 22

Figure 4.2-2: D1, D4 ON for $\phi = 90^0$-plane. 24

Figure 4.2-3: D2, D4 ON for $\phi = 90^0$-plane. 25

Figure 4.2-4: D2, D3 ON for $\phi = 90^0$-plane. 26

Figure 4.2-5: Simulated 3D radiation pattern of the proposed antenna at 5.8-GHz (i) D1, D4 ON (ii) D2, D4 ON (iii) D2, D3 ON (for $\phi = 90^0$). .26

Figure 4.3-1: Optimised parameter of the designed antenna. 28

Figure 4.4-1: Prototype of the proposed antenna (i) Top view, (ii) Bottom view.....29

Figure 4.4-2: Measured and simulated reflection coefficient (i) when D1 & D4 ON; (ii) when D2 & D4 ON; (iii) when D2 & D3 ON. 31

Figure 4.4-3: Measured and simulated radiation pattern for (i) D1 & D4 ON; (ii) D2 & D4 ON; (iii) D2 & D3 ON for at $\phi = 90^0$-plane. 33

Figure 4.4-4: Measured radiation pattern versus frequency of the fabricated prototype antenna (i) State 1, (ii) State 2, (iii) State 3.....35

List of Tables

Table No. **Table Caption** **Page No.**

Table 3.3-1: Parameter List of 5.8-GHz Dual-Beam Switchable Antenna (mm) 15

Table 3.4-1: Comparison between Presented and Preceding Antennas 18

Table 4.3-1: Parameter List of 5.8-GHz Multi-Beam Switchable Antenna (mm) 28

Table 4.4-1: Comparison of the proposed antenna with previously reported antennas. 35

Chapter 1: INTRODUCTION

1.1 BACKGROUND

Wireless communications have seen rapid growth in recent years, leading to the high demand for the unification of multiple wireless quality into smaller equipment such as a reconfigurable antenna. As we desire smaller equipment, reconfigurable antenna with compactness has become high in demand, since the operating frequency, radiation pattern, and polarizations of this type of antenna can be reconfigured according to the system's requirements. However, achieving the desired function for the reconfigurable antenna, successful integration into the required system, and getting the most efficient, cost-effective result is a challenge for antenna designers.

The antenna-array systems provide numerous applications used for wireless communication, such as radars, satellite communication, and other application with high directivity. A beam-steering antenna is one of the well-researched examples of such a configuration. Generally, an array of antenna is used to form and steer a radiated beam of energy. This diverse type of antenna generates a multiplicity of beams with a switchable output to make a signal stronger. The main advantages of reconfigurability are reduced cost, simplicity, and overall volume reduction. Antenna beam steering technology thus, has been used with systems like cellular or mobile telecommunications and in particular 5G as well as many other wireless communications.

1.2 PROBLEM STATEMENT

This paper will focus on beam-steering antenna theory with PIN diodes and 90^0-hybrid coupler. The former design proposes a novel dual-beam switchable array antenna with PIN diodes. The novelty of this design lies in its single feed line, simple layout, and biasing current which ensures the alternate activation of the diodes. A multi-beam array antenna has been proposed as the 2^{nd} design, again, with a single feed technique. The beam-forming network (BFN) of this proposed antenna is realized very easily using hybrid couplers and single-pole double-throw (SPDT) switches.

The main focus of the proposed designs is on simplicity. Most of the previously proposed design, discussed in the literature section, use complex design with multiple feed network to provide multiple beam directions. The designs can cover more areas as they produce more beams, however, the design complexity downgrades the antenna characteristics such as gain and efficiency. As such, this paper proposes simple beam-steering microstrip patch antenna design suitable for various wireless communication application.

1.3 AIMS AND OBJECTIVES

The paper will discuss two significant design with beam-steering characteristic. A beam-switching antenna consists of generating a multiplicity of beam that may be switched on or off according to an algorithm that is able to sense the desired direction of transmission or reception. To achieve a good gain, stable radiation pattern along with simple layout and biasing circuit, the objectives are given below:

- To design array antenna suitable for beam-steering application.
- To optimize single feed line to achieve beam steering performance.
- Use PIN diodes and Hybrid coupler to achieve desired beam directions.

The designed antennas would create dual-beam and multi-beam directions respectively. The feature was achieved using simple electronic components such as PIN diodes and hybrid coupler.

1.4 SIGNIFICANCE, SCOPE AND DEFINITIONS

Two 5.8-GHz simple beam-steering square microstrip array antenna is proposed in this study. The proposed antenna designs use single feed technique to ensure the alternate activation of Diodes, resulting in the beam switching of the positive and negative sides of the radiation pattern. The addition of hybrid coupler elevates the number of beam direction using the switching characteristic of PIN diode, for larger number of array antenna design. The proposed theory is not limited to only 5.8-GHz application and can be applied to a broad range of frequencies keeping its simple design intact.

1.5 THESIS OUTLINE

Chapter 2 reviews the literature background of the study. A discussion of previously proposed antenna and their outcomes are present in this chapter.

Chapter 3 describes the dual-beam switchable array antenna design. The theoretical background, design parameter and antenna characteristic of the dual-beam steering antenna is explained here.

Chapter 4 is based on the multi-beam switchable array antenna. The component and design parameter, their significance, as well as the methodology of this design is presented in this chapter.

Chapter 5 is the conclusion chapter. The future scope of the study will be discussed in this section.

Chapter 2: LITERATURE REVIEW

Beam reconfigurability enables an antenna to radiate different radiation patterns in different directions for a specific frequency [1], [2]. Thus there is no need for multiple antennas to radiate each pattern. Moreover, there is an increase in radiation coverage, channel capacity, and possible point to multipoint communication. [3] utilized beam-forming network (BFN) to produce multi-beam for 5.8GHz frequency. A simple 4 x 2 BFN with a magic-T, 90^0 hybrid coupler, and two single-pole double-throw (SPDT) switches could produce four different beam patterns; sum, difference pattern, and two other beams at -15^0 and $+18^0$. [4]–[6] experimented with millimeter-wave frequency. [4] uses the Butler matrix (BM) frequency diverse retrodirective array (BM-FDRA) technique and focused angle-range beamforming with orthogonal property to serve multiple users simultaneously. Whereas, [5] uses a wideband vertically installed planar transition (VIPT) to implement as many as 32 different beam directions with coverage of 70^0 in terms of elevation and azimuth. [6] uses the simplest technique of using two PIN diodes in the L-shaped stub to produce a 18^0 beam shift. Another instance of using PIN diodes is found in [7] with the addition of transformer oil enabling it to operate at different frequencies according to different oil heights. The four PEC arms ranging from 5.21 GHz to 6.56 GHz house four PIN diodes that provide four different directions. [8]–[10] are some examples of multiple-feed beam-steering antenna designs. The application of these works ranges from mobile devices to 5G applications and satellite applications. The beam angle from the mentioned works varies from 63^0 up to 180^0.

[11] is an example of typical frequency reconfigurable antenna, that can be easily incorporated with beam steer function. In-Band Full-Duplex (IBFD) with high inter-port isolation application using dual-polarized antenna array is presented in [12]. The antenna operating frequency ranges from 2.1 to 2.4GHz and consists of four H-shaped slots, stacked patches with two hybrid coupler. Substrate integrated waveguide (SIW) technique is used to produce a compact 5G beam-steering antenna at 24 GHz in [13]. The output signal can be steered from -29 degrees and +29 degrees. In [14], a survey has been done on different beam-steering technique with the aim of identifying areas of improvements. [15] proposes an innovative design of the Butler matrix to drive patterns of the antenna. The Butler matrix consists of four 90^0 couplers and two broadband stepped 45^0 phase shifters. Two different schemes namely Beam-steering using Hybrid Directional Coupler and Beam Steering using Switched Line Phase Shifter are proposed in [16]. They are specially designed for 5G, S-band applications. A new Active Integrated Array Antenna (AIAA) consisting of a first-harmonic push-push oscillator, four linearly polarized microstrip antenna and a switchable feed network for dual-beam switching is proposed in [17]. The beams of this antenna is found at $\theta = \pm 10°$. In [18], three classes of the latest beam scanning antenna systems; Reflectarrays (RAs), Transmitarrays (TAs), and Near-Field Meta-Steering (NFMS) are designed and discussed. [19] is another work where characteristics and fundamental properties of the reconfigurable antenna, different types of effective implementation techniques for reconfigurable antennas are investigated. Among different techniques, electronic switches are the most popular one due to their reliability and efficiency. [20] provides a work with both frequency and pattern reconfigurability. An Active Frequency Selective Surface (AFSS) with feed antenna is used to achieve this function.

A novel two-layer beam-steering array antenna with a modified 4 x 4 Butler matrix is presented in [21]. There are four novel 90^0 circular patch couplers and two 45^0 half circular patch phase shifter present in the proposed Butler matrix. A system with good directivity, high Isolation and good return loss is proposed in [22]. A steerable 2 x 2 antenna array with a 2 x 2 Butler matrix and a 3-dB quadrature coupler is used for the beam steering function. [23] is a twelve-beam printed patch antenna for pattern reconfigurable application. The patch is fed at four sides with coaxial feeds and diagonal lines of vias are inserted to restrict currents to the edges. [24] is a compact multi-beam 2 x 2 patch array antenna, capable of simultaneously switching the beams among nine different directions as well as reconfiguring polarization between two circular polarization states. A novel leaky-wave antenna (LWA) designed on a substrate integrated waveguide (SIW) with fixed-frequency beam-steering (FFBS) is proposed in [25]. PIN diodes in this design work as binary switches. A dual-beam switchable antenna array at 2.4 GHz with three $0^0/180^0$ couplers and four PIN diodes is presented in [26]. The implemented array gives steering angles of 0^0, $\pm 19°, \pm 31°,$ and $\pm 51°$. The proposed antenna in [27] employs a tunable ground with parasitic steering for the movement of main beam. There are a permanent region and two tunable regions formed from liquid metals in the tunable ground plane. The antenna operates at 5.3 GHz and can provide continuous steering from -30^0 to $+30^0$. Two miniaturized multimode beam-steering antennas with digital and analog beamforming with the $0^0/180^0$ phase switch and variable gain amplifier (VGA) used for Internet of Things (IoT) application are proposed in [28].

In this paper, the beam-forming network (BFN) consists of PIN diodes and 90^0 hybrid couplers. PIN diodes ensure the smooth transition of electrical switching, thus decreasing the number of feeding ports. The PIN diodes are used in a number of areas due to its structure proving some properties having

particular use. The PIN diode can be used as a high voltage rectifier as the intrinsic region provides larger separation between the P an N junction. This allows the toleration of higher reverse voltages. The property that is used in the discussed antenna design in this paper is the use of RF switch. The intrinsic layer increases the distance between P and N region helping them to act as a switch. The increased distance has a reverse effect on capacitance, thereby increases the level of isolation when the diode is in reverse biased state. The other electrical components inductor and capacitor are also highly configurable with antenna based application. The inductor in antenna mostly maintain the operating frequency and prevent fluctuation in current flow. The most common applications of capacitors in antenna are impedance matching, frequency tuning, filtering etc. It also ensures that no unwanted bias current is flowed to the antenna system.

On the other hand, the hybrid coupler is a four-port symmetric device that can split the power equally with a 90^0 phase shift between them. Moreover, this type of coupler is designed to be highly symmetrical meaning any port can be taken for the input power and the result will be the same. More about hybrid couplers can be found in [29], [30] . This type of device is widely used to combine or split signals in amplifiers, switching circuits and beam-forming antenna network in a wide range. Military applications where power or frequency need to be monitored or controlled, hybrid coupler is an essential device for that.

This paper cover two different types of Beam switching antenna. The former describes a dual-beam switchable array antenna with PIN diodes. The specialty of this design lies in its single feed line simple layout and biasing circuit. The PIN diodes ensures the alternate activation of diode and the beam switching in the positive and negative side of the radiation pattern. The later proposed antenna is designed at 5.8 GHz with a single feed technique and two

90^0 hybrid couplers. The four PIN diodes are responsible for three different beam directions. Compared to the hybrid coupler designs implemented in [12-16], the proposed design uses the most straightforward design. The single feed network ensures the activation of two single-pole double-throw (SPDT) switches. This results in the beam as positive, negative, and sum beam of the radiation pattern.

Chapter 3: DUAL-BEAM SWITCHABLE ARRAY ANTENNA

3.1 ANTENNA STRUCTURE

The schematic layout and cross-sectional view of the presented dual-beam switchable array antenna are shown in Figure 3.1-1 There are three square patch antenna elements that are placed at a uniform distance from each other. A switchable feed network is used to provide not only an RF signal to the antenna elements but also a switching voltage for the diodes. Though the distance among the three square patch elements is uniform, the distance from the microstrip junction to the patch element varies with their position. The leftmost patch #2 and rightmost patch #3 have similar distances "a" from the microstrip feed junction. However, the centre patch and the junction are kept at a distance "b". The difference in length between "a" and "b" creates a phase difference between the antenna elements. Two PIN diodes, D1 and D2, are also added to the design which is placed as an anti-parallel arrangement. This arrangement ensures the alternate activation of the PIN diodes. The diode activation also impacts the activation of the leftmost patch #2 and rightmost patch #3. To ensure that the diode is electrically connected to the patch, vias are added at the centre of patch #2 and patch #3.

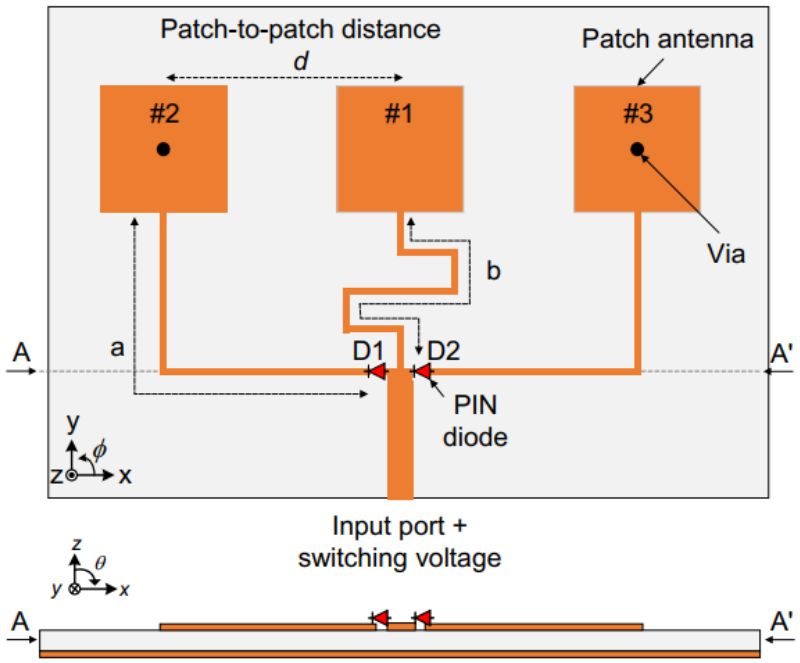

Figure 3.1-1: Structure design of the proposed 5.8-GHz single-feed dual-beam switchable array antenna

3.2 OPERATING PRINCIPLE

3.2.1 PIN Diode

The PIN diode consists of heavily doped P and N regions separated by intrinsic 'I' region as shown in Figure 3.2-1 In forward-bias, it follows the principle of semiconductor diode and acts like a current controlled variable resistance. During reverse-biased, the device acts like a constant capacitance.

In principle, there is no difference between a normal diode and a PIN diode. The only difference lies in the addition of undoped intrinsic region. In normal diode, a depletion region exists between the P and N regions due to the diffusion characteristic of the unbalanced charge between these two region. The depletion region is created during unbiased state for a normal diode. Similar to normal diode, PIN also has a depletion region within itself, and when the diode is forward biased, the carriers enter the depletion region and the two types of

carrier meet starting the current flow. When, the diode is forward biased, the carrier concentration, that is holes and electrons is very high compared to the intrinsic level carrier concentration. Due to the high injection level of carrier and the narrow thickness of the intrinsic region, the electric field can deeply extend into this region covering almost the entire length. This electric field then helps in speeding up the transfer of the charged carriers from P to N region. This results in faster diode operation and advantageous for high frequency operation. This type of diode is generally made of silicon. The intrinsic region of the PIN diode acts as an inferior rectifier thus, used in various devices such as attenuators, photodetectors, fast switches, high voltage power circuits etc. The fast switching characteristic of PIN diode is the reason why it is suitable to use in antenna design.

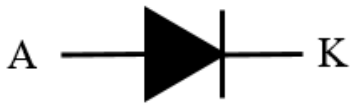

(i)

(ii)

Figure 3.2-1: PIN Diode (i) symbol, (ii) structure

3.2.2 Proposed Antenna

Figure 3.2-2 exhibits the fundamental theory of the prospective antenna's concept. The gap between two antenna elements is denoted by ‘d’. θ and ‘A’ are the angle of the radiated Radio Frequency wave and the amplitude of an input signal, respectively. The array factor is calculated from the following equations.

$$f(\theta) = \sum_{n=1}^{2} I_n \, e^{[j(n-1)(kd\sin\theta)]} \quad (1)$$

where I_n and k are the complex amplitude of the nth element and free space wave number. Besides, 'd' represents the distance between the microstrip patches. If the signal is supplied through the Port,

$$f(\theta) = \frac{A}{\sqrt{2}} e^{(-j\frac{\pi}{2})} + \frac{A}{\sqrt{2}} e^{j(kd\sin\theta)}$$

$$f(\theta) = \frac{A}{\sqrt{2}} e^{(-j\frac{\pi}{2})}[1 + e^{k(kd\sin\theta+\frac{\pi}{2})}] \quad (2)$$

The f(θ) or array factor of the antenna will be maximum if $e^{k(kd\sin\theta+\frac{\pi}{2})} = 1$. Therefore,

$$kd\sin\theta + \frac{\pi}{2} = 0,$$

$$\sin\theta = -\frac{\frac{\pi}{2}}{kd}, k = \frac{2\pi}{\lambda}$$

Where λ is the wavelength and then

$$\theta = \sin^{-1}\frac{\lambda}{4d} \quad (3)$$

According to the equation (3), at the angle of -16^0, the peak is found for the frequency of 5.8 GHz with a 46-mm antenna separation. More detailed analysis can be found in [28].

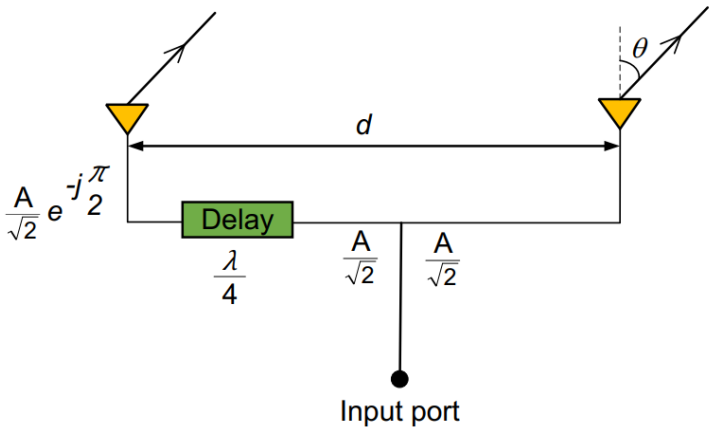

Figure 3.2-2: Fundamental theory of the proposed antenna

The 3D radiation patterns are shown in Figure 3.2-3 at 5.8-GHz designed frequency, where the green lines at the center of the 3D patterns represent the cutting planes of the antenna. Advanced Design System (ADS) Momentum of Keysight Technologies' is used to produce these 3D radiation patterns. The main beam tilts to $\theta = \mp 13°$ in the $\phi = 0^0$-plane for diode D1 and D2 ON condition, respectively. In the $\phi = 90^0$-plane, for both diode conditions, the radiation patterns are almost identical.

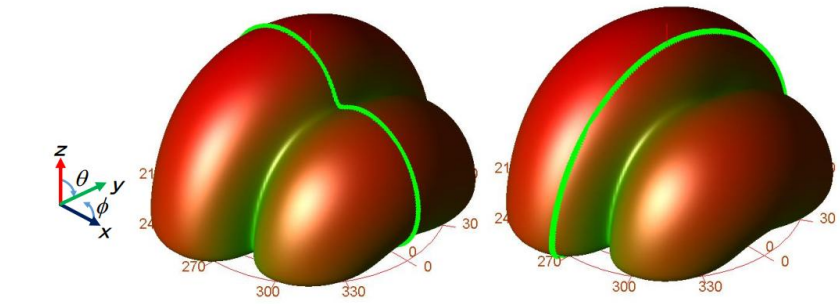

(i) (ii)

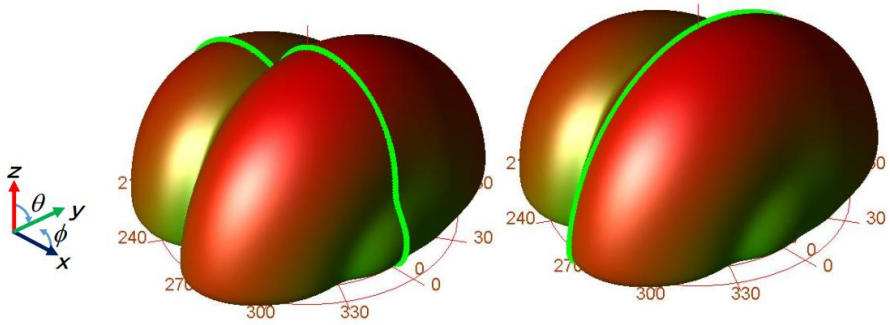

(iii) (iv)

Figure 3.2-3: Simulated 3D radiation pattern of the proposed array antenna at 5.8-GHz, (i) D1 ON ($\phi = 0^0$). (ii) D1 ON ($\phi = 90^0$). (iii) D2 ON ($\phi = 0^0$). (iv) D2 ON ($\phi = 90^0$).

3.3 DESIGN

Figure 3.3-1 shows the optimized parameters of the proposed antenna for 5.8-GHz. Here, L, W, d, and Z act for length, width, patch separation, and impedance, respectively. The ground size of the proposed antenna is 60 mm (L_1) x 130 mm (W_1). Three square patch antennas with 16.8 mm (L_2) dimension are placed with 0.94 λ (=46 mm) separation. The 0.7 mm (W_2) microstrip feed line is utilized from the center patch antenna to the microstrip line junction. The distances from the center and left or right antenna elements to the microstrip junction are 55.7 mm (b) and 63.7 mm (a), respectively. To insert the PIN diodes, 0.4-mm (g) gaps are used. A 50Ω (Z_0), 2.4-mm (W_3) microstrip line is designed from the input port to the microstrip junction. The proposed antenna is etched on a polytetrafluoroethylene (PTFE) substrate with a permittivity of 2.15 and a thickness of 0.8-mm. The proposed antenna is simulated by using two electromagnetic field simulation software; Advanced Design System (ADS) Momentum and SIMULIA CST Studio Suite.

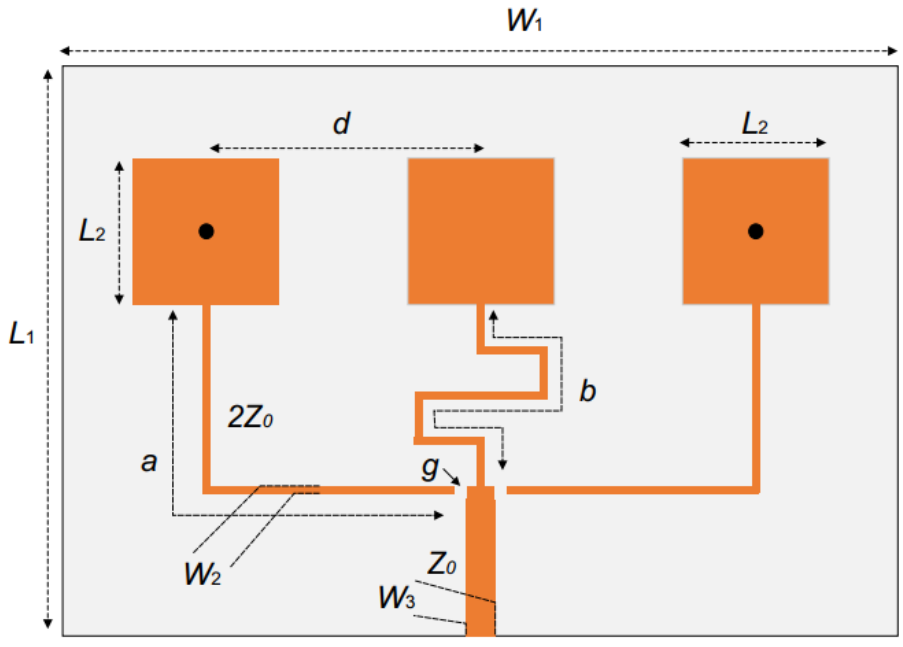

Figure 3.3-1: Optimized parameters of the proposed antenna.

The below table denotes the parameter list of the proposed antenna design.

Table 3.3-1: **Parameter List of 5.8-GHz Dual-Beam Switchable Antenna (mm)**

L_1	60	W_3	2.4
W_1	130	a	63.7
L_2	16.8	b	55.7
W_2	0.7	Z_0	50Ω
d	46	g	0.4

3.4 ANTENNA PERFORMANCE

Figure 3.4-1 presents the photographs of the 5.8-GHz prototype of the proposed antenna. The antenna size is 60 mm x 130 mm. Patch antennas, microstrip lines, and PIN diodes are printed at the upper side of the substrate. Via is used at the center of the left and right antenna elements to provide grounding for the PIN diode. In the prototype, Skywork's DSG9500-000 PIN diode is used. Positive (+0.9V, 0.10mA) and negative (-0.9V, 0.10mA) biasing are used to turn on the PIN diodes D1 and D2, respectively.

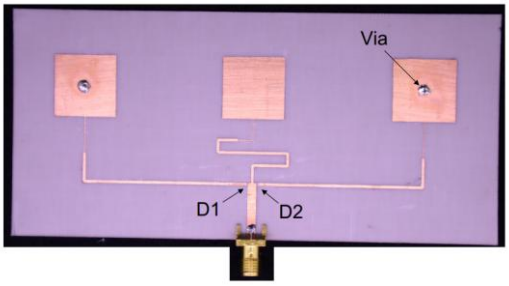

(i)

(ii)

Figure 3.4-1: Fabricated prototype of the presented 5.8-GHz dual-beam switchable single-feed antenna array. (i) Top view. (ii) Bottom view.

The measured and simulated reflection coefficient of the proposed antenna is shown in Figure 3.4-2 The simulated reflection coefficient in CST shows a lower operating frequency than the ADS. The measurement gives a bandwidth of 200MHz (3.5%) at 10-dB point. Both diode conditions provide almost identical performance.

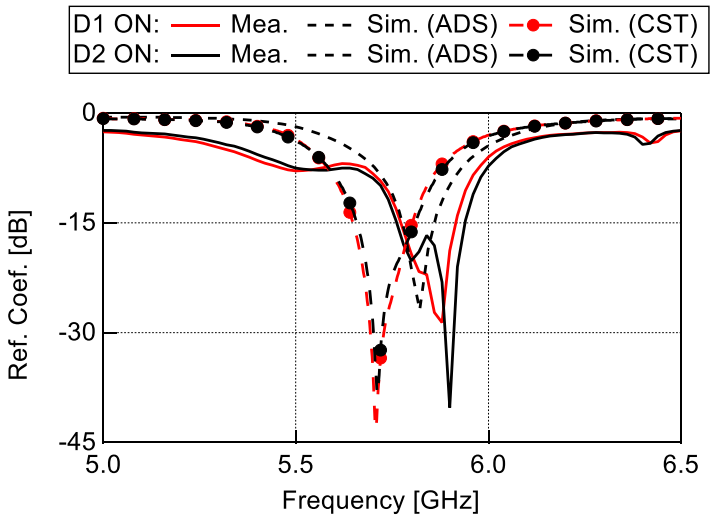

Figure 3.4-2: Measured and simulated reflection coefficient.

Figure 3.4-3 and 4 depict the normalized measured and simulated radiation patterns for ADS and CST of the proposed design for diode D1 and D2 ON conditions, respectively. The performances of the antenna are analysed at the frequency of 5.8GHz. Here, the measured and simulated results are

represented using the solid and dashed lines, respectively. Besides, red color is used for co-polarization and black is for cross-polarization radiation pattern. The cross-polarization suppression for both simulation and measurement is better than 15dB as appeared in the figures which indicate satisfactory performance by the presented antenna. The measured results are found to be well-matched with the simulated results. The measured peak gain is 8.9dBi at $\phi = 0^0$-plane and 6.3dBi at 90^0-plane for D1 ON condition. On the other hand, for D2 ON condition, around 8dBi and 6.2dBi peak gains are found for $\phi = 0^0$ and 90^0-planes, respectively. These values are 1.5dB lower than the ADS simulation result. For both conditions, the beam is found to be tilted at $\theta = \pm 12°$ at $\phi = 0^0$-plane in the measurement compared to the ADS $\pm 13°$ and CST $\pm 8°$.

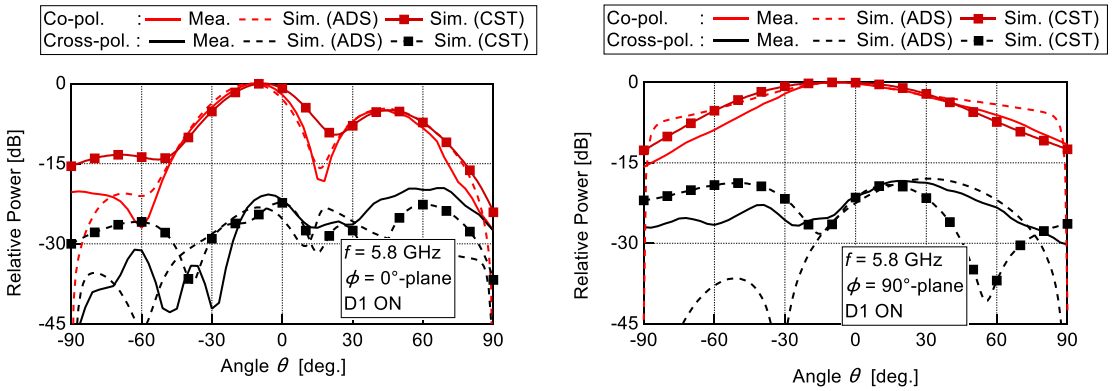

(i) (ii)

Figure 3.4-3: Measured and simulated radiation patterns for D1 ON condition. (i) $\phi = 0^0$-plane. (ii) $\phi = 90^0$-plane.

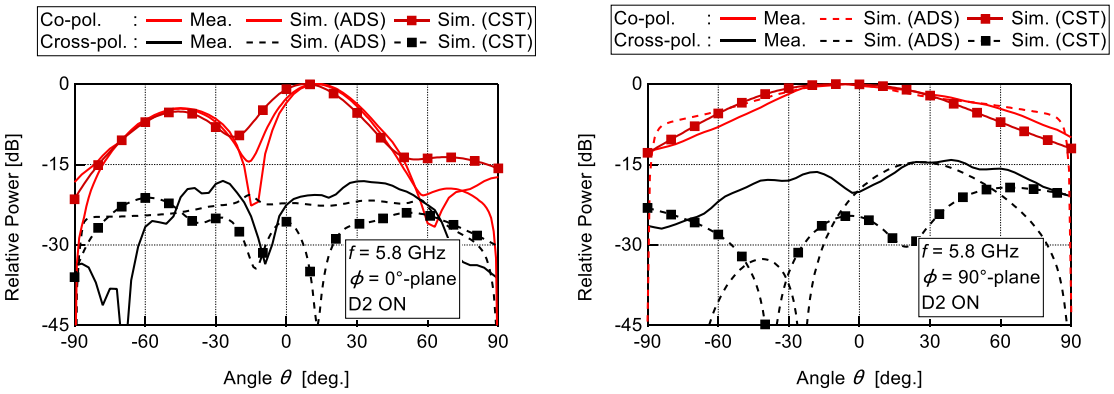

(i) (ii)

Figure 3.4-4: Measured and simulated radiation patterns for D2 ON condition. (i) $\phi = 0^0$-plane. (ii) $\phi = 90^0$-plane.

Table 3.4-1: Comparison between Presented and Preceding Antennas

[Ref.]	Freq. [GHz}	Imp. BW. [GHz]	No. of ant. elements	Isolation [dB]	Gain for condition 1 [dBi]		Gain for condition 2 [dBi]	
					$\phi = 0^0$	$\phi = 90^0$	$\phi = 0^0$	$\phi = 90^0$
[31]	5.8	1.30	4	17	10.7	68.4	10.4	7.9
[32]	4.7	3.90	1	17.2	<4.4		<4.4	
[33]	2.2	0.58	4	80	>3.9	>3.9	>3.9	>3.9
[34]	2.4	0.015	4	50	1		-1.3	
[35]	2.4	0.20	4 main & 4 parasitic	80	9.6	9.6	9.6	9.6
Proposed	5.8	0.20	3 (2 active)	-	8.9	6.3	8.0	6.2

Chapter 4: MULTI-BEAM SWITCHABLE ARRAY ANTENNA

4.1 ANTENNA STRUCTURE

Fig 4.1 (a) shows the block diagram of the proposed 5.8-GHz antenna. The design will provide three beam direction conditions. This design consists of four square patch antennas, two sets of hybrid couplers, two sets of single-pole double-throw (SPDT) switches, and a single port. The SPDT switch consists of two PIN diodes with opposite directions. One hybrid coupler and one single-pole double-throw (SPDT) switch make up a switched-line phase shifter unit. Activation of the SPDT switch denotes the input port of the hybrid coupler. Due to the symmetric characteristic of the hybrid coupler, the arms connected to Port 1 can alternatively act as input ports thus exciting the associated patch along with it. This alternate activation of the SPDT switch and hybrid coupler ensures the different beam directions.

Fig 4.1 (b) shows the schematic layout and cross-sectional view of the proposed multi-beam switchable array antenna. The four square patch antenna elements are placed at a uniform distance 'd' from each other to reduce the side lobe of the radiation patterns. Patch #1, #2, and #3, #4 are connected to two 90^0 hybrid couplers. Each input and isolated leg of the hybrid coupler has PIN diodes D1, D2, D3, and D4 attached. These legs of hybrid couplers then create a square shape such that each leg maintains a uniform distance from the feed junction. A single feed network responsible for the RF signal creates a microstrip T-junction at the center of the square shape. A capacitor is added to the feed line and an inductor is added at the T-junction end of the feed line. Two voltage sources V_{BIAS1} and V_{BIAS2} are added at the center of patches #1 and #4 to provide switching voltage for PIN diodes, capacitor, and inductor

respectively. By activating any two PIN diodes, a phase difference is created among the antenna elements. Diode pairs D1, D4 and D2, D3 are in the opposite

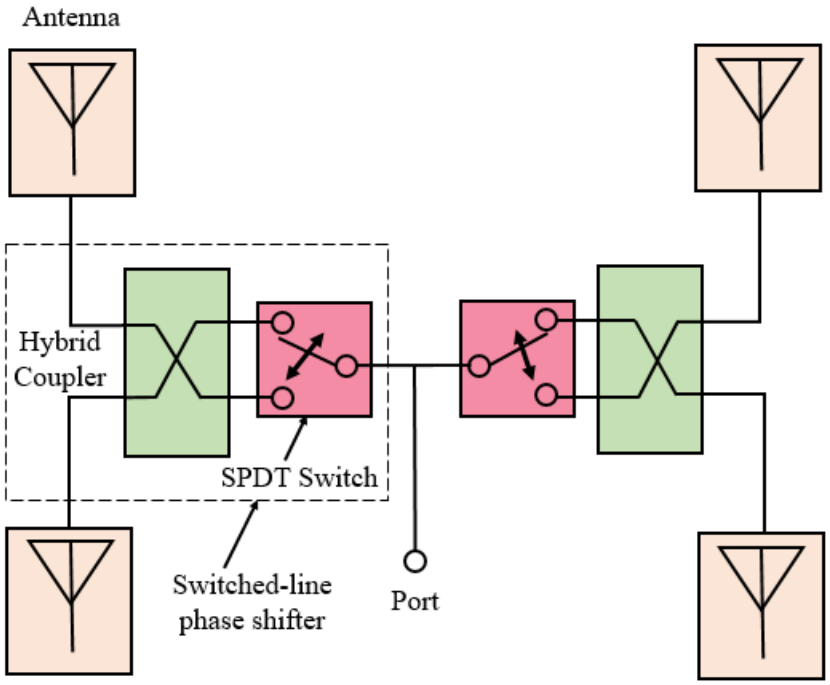

Figure 4.1-1: Block Diagram of the proposed three-state pattern reconfigurable antenna.

direction of each other. Diodes D1, D2 are placed such that they are parallel to diodes D3, D4. This arrangement ensures the alternate activation of the parallel pair of PIN diodes. The alternate activation of the diode sets works similarly to a single-pole double-throw (SPDT) switch. Thus, D1, D2, or D3, D4 and a hybrid coupler create a switched-line phase shifter unit. Patches #1, and #2 can be activated either by D1 or D2. Similarly, patches #3 and #4 can be activated by both D3 and D4. Finally, to ensure that the PIN diodes are electrically connected to the patches, via is added at the end of the inductor.

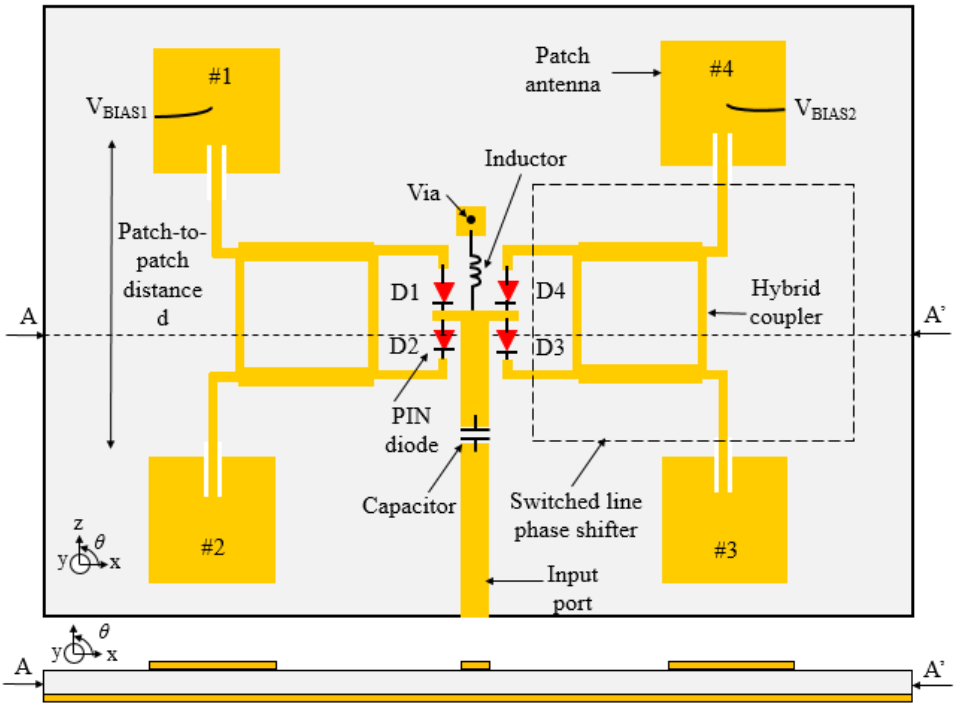

Figure 4.1-2: Schematic layout and cross-sectional view of the proposed 5.8-GHz multi-beam array antenna.

4.2 OPERATING PRINCIPLE

4.2.1 Hybrid Coupler

The 90^0 hybrid coupler is a 3 dB directional coupler with a symmetric characteristic. The output ports are called Through and Coupled arms. The output ports are always situated at the opposite sides of the Input port, thus, the last port becomes isolated hence the name Isolated port. This device is also known as branch line coupler. Figure 4.2-1 shows the structure of the hybrid coupler. The scattering matrix S is given below proving the symmetry of the hybrid coupler

$$S = \frac{-j}{\sqrt{2}}\begin{pmatrix} 0 & j & 1 & 0 \\ j & 0 & 0 & 1 \\ 1 & 0 & 0 & j \\ 0 & 1 & j & 0 \end{pmatrix} \quad (4)$$

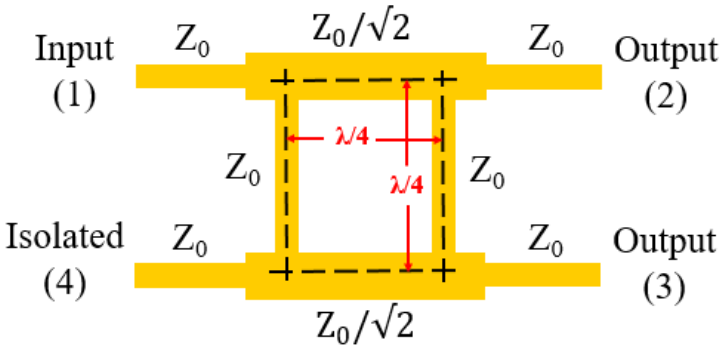

Figure 4.2-1: Structure of 90^0-hybrid coupler.

The Figure 4.2-1 shows a four port device. The input is at port 1 and output ports are 2 and 3, remaining port 4 becomes isolated. Alternatively, port 4 can be taken as input port and port 1 becomes the isolated port. The output ports stay unchanged. Hybrid coupler operation is not affected when the ports are interchanged with ports 2 and 3 because of the high degree of symmetry. Same for ports 1 and 4, depending on suitable operation any of them can be input and isolated port.

The main characteristic of hybrid coupler is that they will split the input signal in half or combine the input signal and create a 90^0 phase shift between the output ports. Inconsistency may occur in port 4 due to the patch returns to the absorbing load. The impedance of all four port are kept at Z_0. The path $Z_0/\sqrt{2}$ is responsible for the split of signal. Then signal is fed through port 1, the direct opposite port 2 becomes through and the other port 3 on the same side becomes coupled port. As the signal travels through a $\lambda/4$ distance from port 1 to port 2 and the width of that path is $Z_0/\sqrt{2}$, the signal found at port 2 will be have half the input signal with 90^0 out of phase. The other half of the input signal will travel through additional $\lambda/4$ distance and reach port 3. Thus it will have half the input signal and will be 180^0 out of phase. The final phase difference of the ports 2 and 3 thus becomes 90^0, hence the name of the hybrid coupler.

4.2.2 Proposed Antenna

The designed antenna will work for three unique conditions. For each condition, two PIN diodes are turned ON while the other two are OFF. This can be achieved as each PIN diode is attached to a separate arm of the hybrid coupler and work as a part of the SPDT switch. They maintain a uniform distance from the T-shaped feed junction to the hybrid coupler arm. Each inactive PIN diode on the arm works as an open circuit since the distance between each hybrid coupler arm and the T-shaped feed junction is **λ**/4. As a result, the antenna reflection coefficient is unaffected by the alternate activation of the diode.

The placement of hybrid couplers between the two sets of antenna arrays leads to a 90^0 phase difference. Due to this phase difference between antenna arrays, the degree of main beam tilt can be calculated by

$$\theta_m = \pm \sin^{-1}\left(\frac{\lambda_0 \Delta\varphi}{2\pi d}\right) \quad (5)$$

here, θ_m, λ_0, $\Delta\varphi$, and d are beam angle, free space bandwidth, the phase shift between antenna elements, and patch spacing respectively. Thus, the main beam can be tilted in the positive, and negative direction as well as stay at the middle position of the x-axis as a sum pattern by alternatingly turning ON and OFF the PIN diodes. More details regarding the equation can be found in [17].

Condition 1: Positive θ_m

When the signal is fed from Port 1, diodes D1 and D4 are turned ON as shown in Figure 4.2-2. The associated arms of the hybrid coupler thus start to act as the input port of the couplers. The remaining arm on the same side of the input arm automatically become the isolated arm. Now the signal goes through the path of D1 and D4. The patches #1 and #2 as well as #3 and #4 each receive half of the input signal as they get splitted in half due to the characteristic of

hybrid coupler. Another characteristic of hybrid coupler creates a 90^0 phase difference between patches #1 and #2; patches #3 and #4. Thus from Fig 6, it is clearly seen that there is positive 90^0 phase difference between the antenna pairs, that is, patches #1, #4 and patches #2, #3 as D1 and D4 are activated. Thus the beam is tilted at the positive plane of the radiation pattern for $\phi = 90^0$-plane.

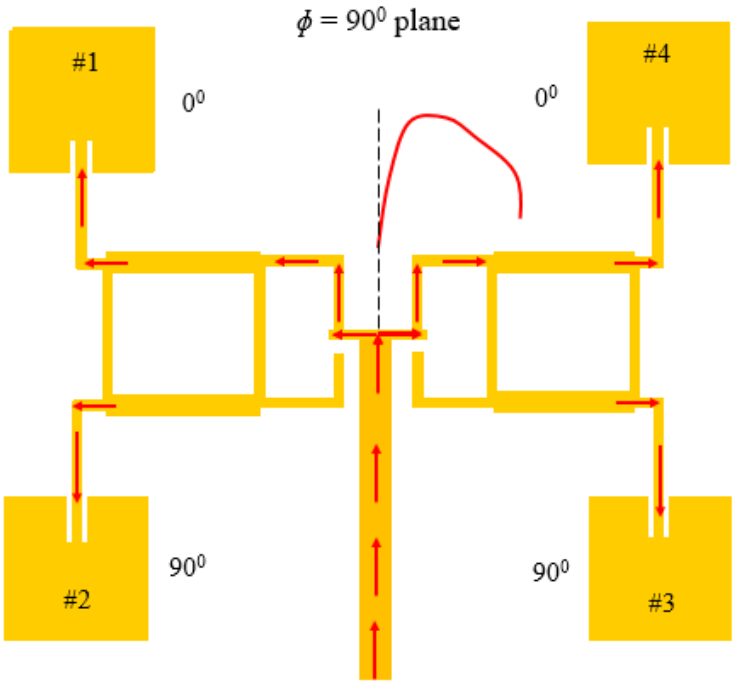

Figure 4.2-2: D1, D4 ON for $\phi = 90^0$-plane.

Condition 2: $\theta_m = 0^0$

The T-junction feed line turns on diodes D2 and D4 in the state. From Figure 4.2-3, the signal travels through a diagonal path and thus patches #2 and #4 have same phase becoming a pair whereas patches #1 and #3 having same phase create another pair. The phase difference of these two pair ultimately become 0^0. Thus, a difference beam is found at the center of the radiation pattern as a sum pattern shown in Figure 4.2-3. Each patch will again receive half of the input signal.

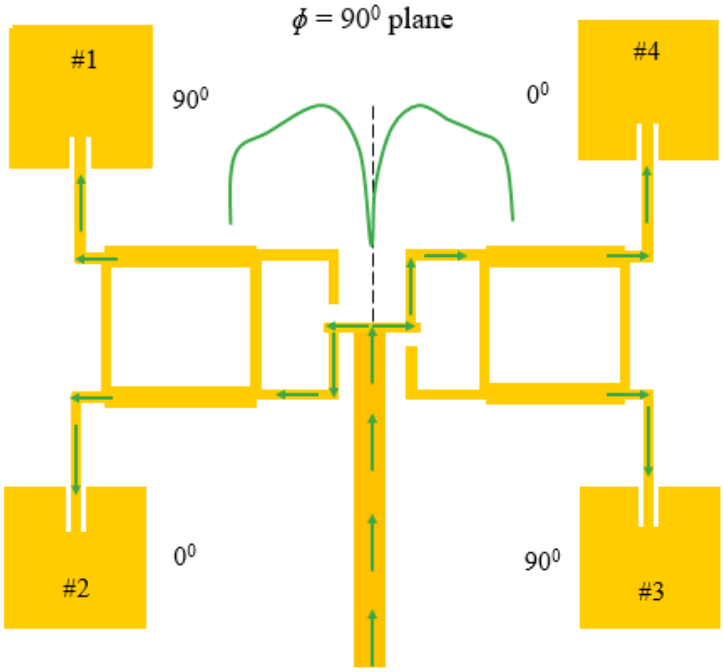

Figure 4.2-3: D2, D4 ON for $\phi = 90^0$-plane.

Condition 3: Negative θ_m

Similar to condition 1, the signal is fed from Port 1, and D2, D3 diodes are turned ON as shown in Figure 4.2-4. The patches again receive half of the input signal and the pairs of antenna array create a phase difference of 90^0. In this condition too, there exist an isolated arm at the same side of the input arm of the hybrid coupler. As D2 and D3 diodes are activated, the phase difference between the patches #2, #3 and patches #1, #2 becomes negative 90^0. Thus the resulting beam is shifted to the negative side of the radiation pattern for $\phi = 90^{0-}$ plane.

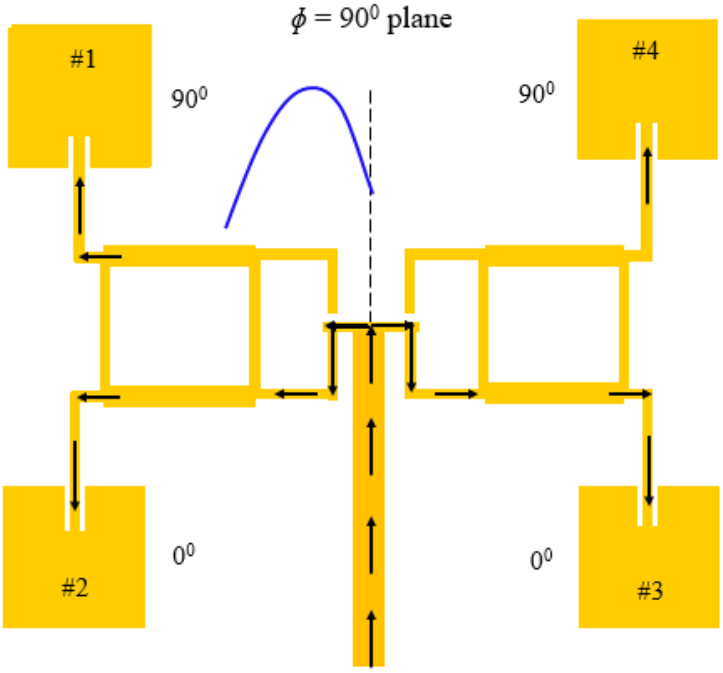

Figure 4.2-4: D2, D3 ON for $\phi = 90^0$-plane.

Figure 4.2-5 represents the 3D radiation pattern of the prospective 5.8-GHz antenna using Keysight Technologies' Advanced Design System (ADS) Momentum. The green lines in the middle of the 3D patterns show the cutting planes of the antenna. The main beam is tilted to $\theta = 14^0$ when D1, D4 are turned ON and $\theta = -14^0$ when D2, D3 are ON; both conditions are found for $\phi = 90^0$ plane. The main beam is found at $\theta = 0^0$ when D2 and D4 are ON for $\phi = 90^0$ plane.

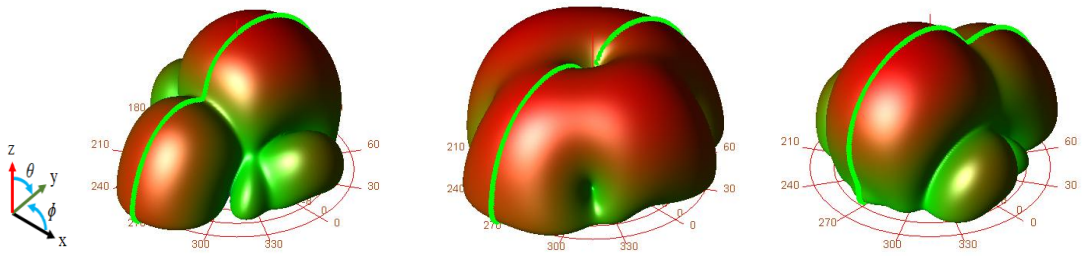

(i) (ii) (iii)

Figure 4.2-5: Simulated 3D radiation pattern of the proposed antenna at 5.8-GHz (i) D1, D4 ON (ii) D2, D4 ON (iii) D2, D3 ON (for $\phi = 90^0$).

4.3 DESIGN

Figure 4.3-1 shows the optimized layout of the designed antenna. Here, L, W, Z, and d represent length, width, impedance, and patch-to-patch distance respectively. The proposed antenna is excited at 5.8 GHz and the wavelength, λ = 51.7mm. The ground size of the proposed antenna is 75 mm (L_1) x 75 mm (W_1). Four square patch antennas with 16.8 mm (L_2) dimension are placed with a 0.81λ (d = 42 mm) separation. As the antenna edge tends to have high impedance, a microstrip line with W_2 (0.7mm) width is added to each output arm of the coupler. Each input arm and isolated arm of the hybrid coupler is connected to a microstrip line of 0.7 mm (W_2) width and 9.84 mm (L_4) length creating a square shaped junction. A 50-Ω (Z), 2.4 mm (W4) microstrip line is added at the center of the square-shaped junction to feed through the input port. The width and length of the arms of the hybrid coupler are W_3 (1.3 mm), W_2 (0.7 mm), L_3 (9.6 mm), and L_4 (9.87 mm) respectively. Z_0 denotes the arm impedance of the hybrid coupler. To insert the PIN diodes, capacitor and inductor, 0.2-mm (g) gaps are used. The proposed antenna is printed on a 0.8 mm thick polytetrafluoroethylene (PTFE) substrate having a permittivity of 2.15. The perspective antenna is simulated by Keysight Technologies' Advanced Design System (ADS) Momentum.

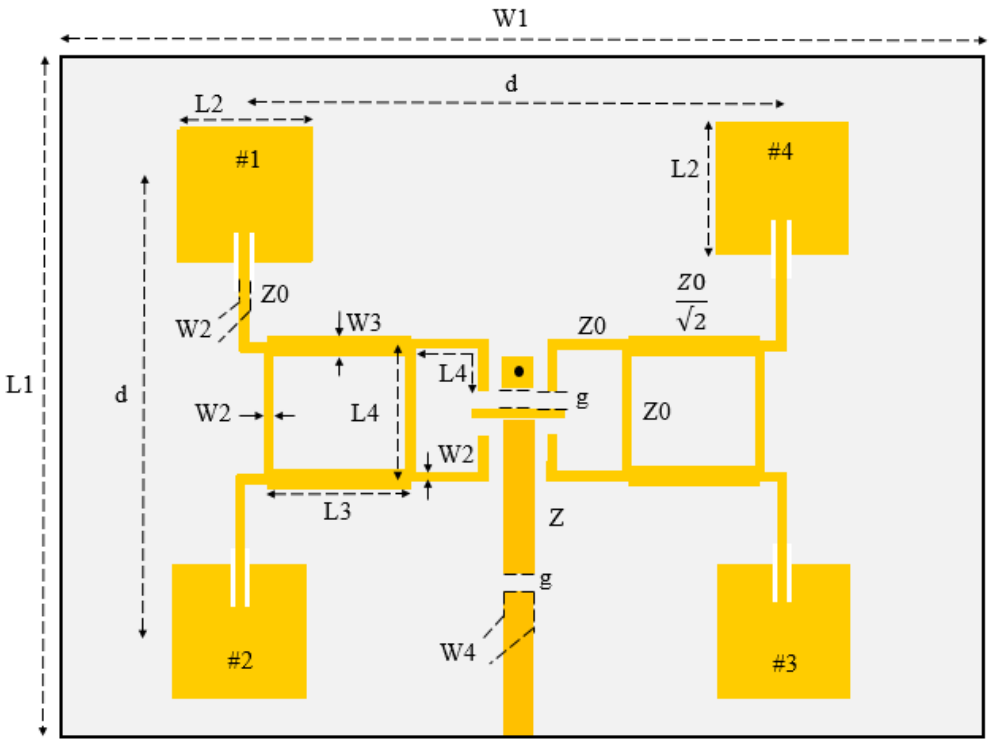

Figure 4.3-1: Optimised parameter of the designed antenna.

The Table 4.3-1 denotes the fabricated parameter list of the proposed antenna in case II:

Table 4.3-1: Parameter List of 5.8-GHz Multi-Beam Switchable Antenna (mm)

L_1	75	L_4	9.84
W_1	75	W_4	2.4
L_2	16.8	g	0.2
W_2	0.7	Z_0	100 Ω
L_3	9.67	Z	50 Ω
W_3	1.3	d	42

4.4 ANTENNA PERFORMANCE

Figure 4.4-1 shows the photographs of the 5.8-GHz fabricated prototype of the proposed antenna. The size of the patch antenna is 75 mm x 75 mm. Patch antennas, microstrip lines, capacitor, inductor, voltage sources, and PIN diodes are placed at the top side of the substrate. Via is added for PIN diode to provide grounding to them. In the prototype, Skyworks's DSG9500-000 PIN diodes, a 4pF capacitor, and a 12nH inductor are used. Two voltage sources VBIAS1 and VBIAS2 are added to provide switching voltage to the active and passive components.

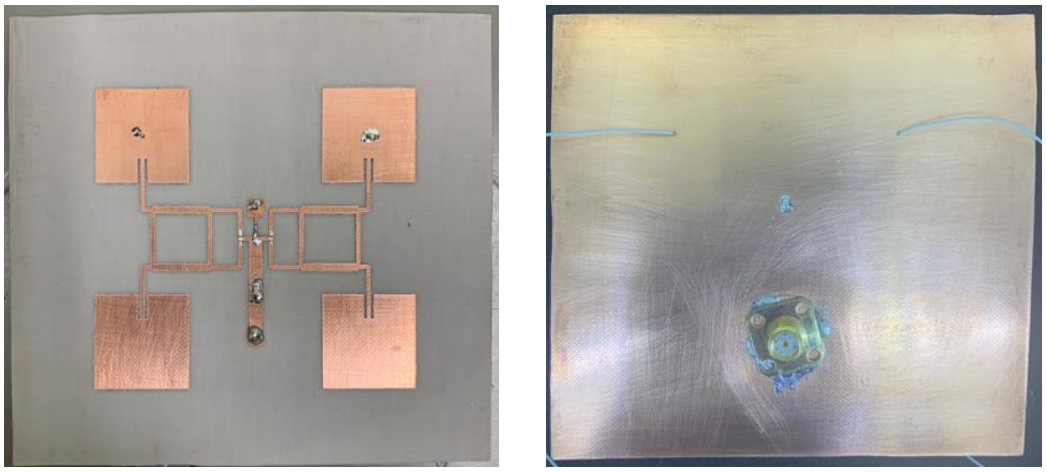

(i) (ii)

Figure 4.4-1: Prototype of the proposed antenna (i) Top view, (ii) Bottom view.

Figure 4.4-2 denotes the measured and simulated reflection coefficient of the proposed antenna. The three colours represent the three state of this design. Solid colour is used to present measured value whereas dashed line represents simulated value. Red colour portrays Condition I that is D1 and D4 ON condition; Black colour is used for Condition II, D2 and D4 active; finally, Blue colour presents Condition III when D2 and D3 are ON. The measured 10-dB

impedance bandwidth of the antenna is around 200 MHz for all three conditions.

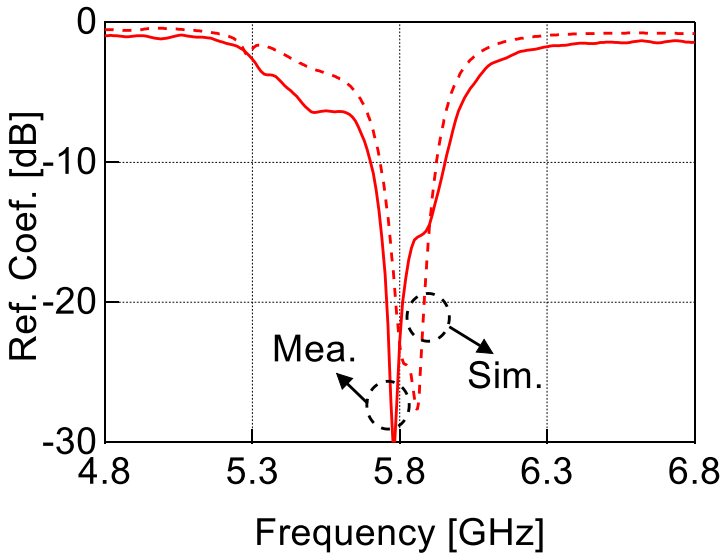

(i)

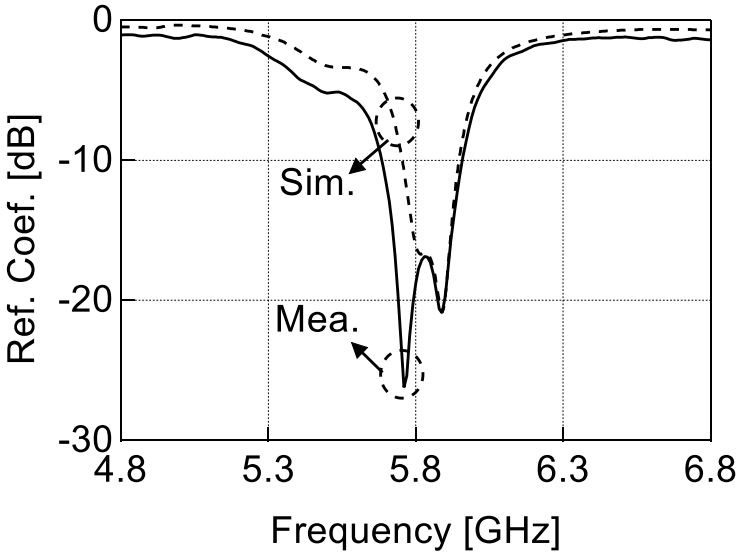

(ii)

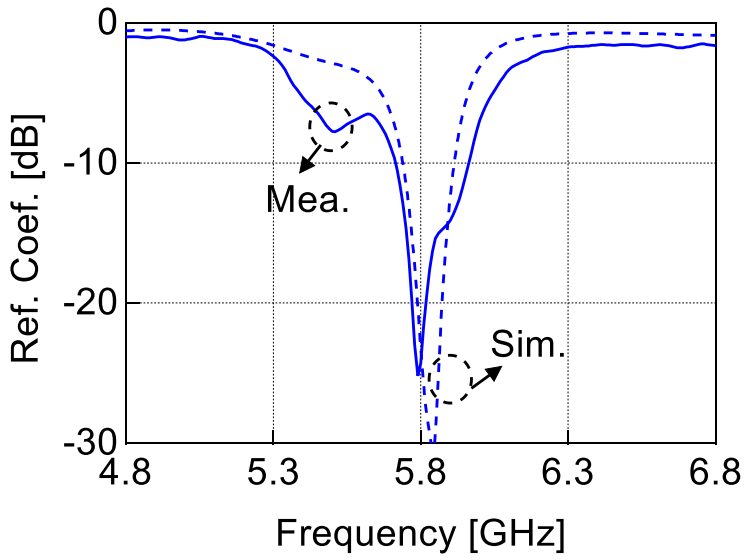

(iii)

Figure 4.4-2: Measured and simulated reflection coefficient (i) when D1 & D4 ON; (ii) when D2 & D4 ON; (iii) when D2 & D3 ON.

Figure 4.4-3 depict the normalized measured and simulated radiation patterns for ADS of the three conditions, respectively. The performances of the antenna are analysed at the frequency of 5.8GHz. Here, the measured and simulated results are represented using the solid and dashed lines, respectively. Besides, red, green and blue are used for co-polarization of different state and black is used for cross-polarization radiation pattern. The cross-polarization suppression for both simulation and measurement is better than 15dB as appeared in the figures which indicate satisfactory performance by the presented antenna. The measured results are found to be well-matched with the simulated results. The measured peak gain is 13.24 dBi at $\phi = 90^0$-plane for D1, D4 ON condition. For D2, D4 ON condition, around 9.04 dBi peak gain is found for $\phi = 90^0$-planes. For the third condition, when D2 and D3 are on, the peak measured gain is about 12.82 dBi. For the three conditions, the beam is found to be tilted at $\theta = \pm 14°$ and 33^0 at $\phi = 90^0$-plane.

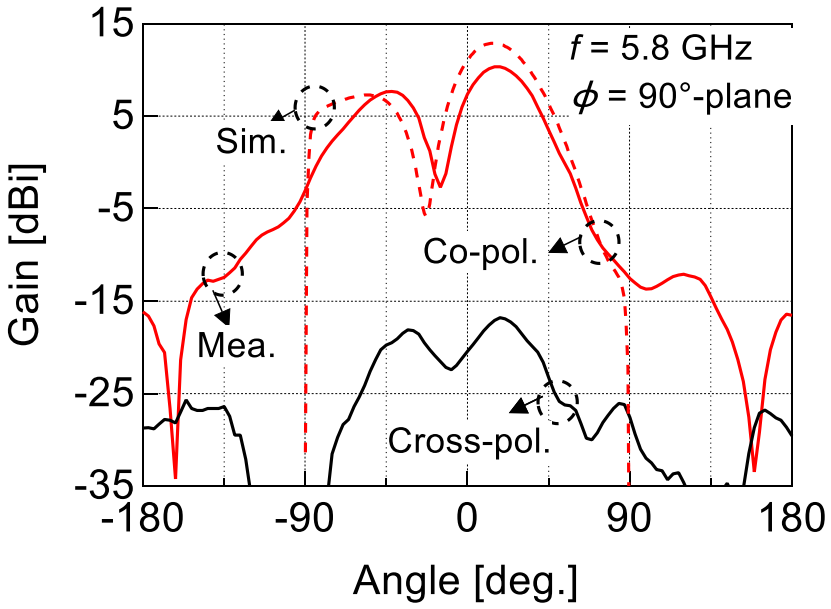
f = 5.8 GHz
ϕ = 90°-plane
Sim.
Mea.
Co-pol.
Cross-pol.
Gain [dBi]
Angle [deg.]
15
5
-5
-15
-25
-35
-180
-90
0
90
180

(i)

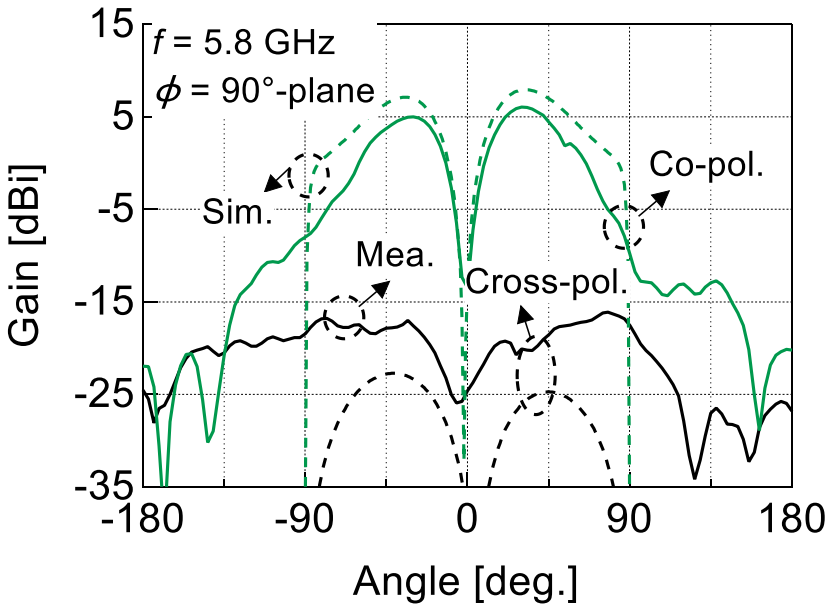
f = 5.8 GHz
ϕ = 90°-plane
Sim.
Mea.
Co-pol.
Cross-pol.
Gain [dBi]
Angle [deg.]
15
5
-5
-15
-25
-35
-180
-90
0
90
180

(ii)

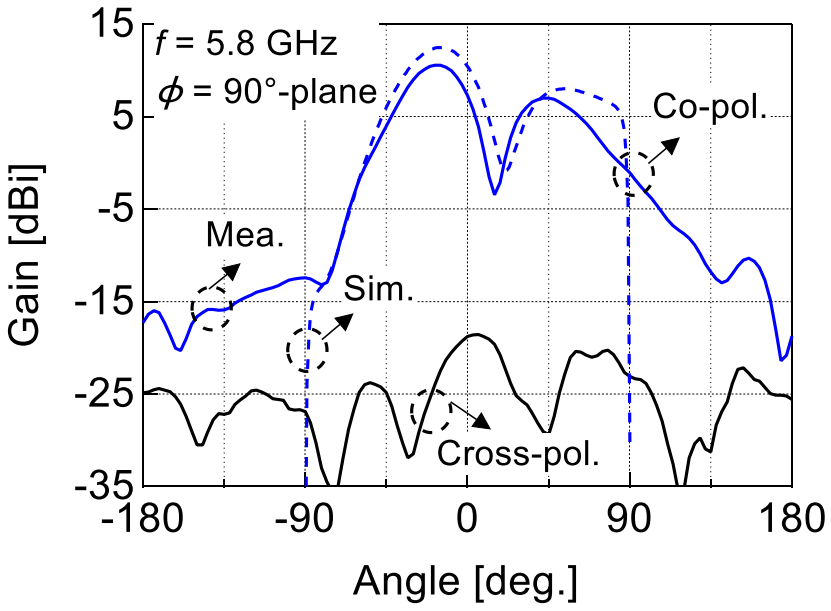

(iii)

Figure 4.4-3: Measured and simulated radiation pattern for (i) D1 & D4 ON; (ii) D2 & D4 ON; (iii) D2 & D3 ON for at $\phi = 90^0$-plane.

Figure 4.4-4 denotes the measured radiation pattern versus the frequency of the prototype antenna. Here, the intensity defines the realized gain of the prototype antenna. It is evident from Figure 4.4-4 (i) that the maximum peak angle occurs at $\theta > 0^0$. As the 90^0 phase shifter has a dependency on frequency, the maximum peak angle varies with frequency. In the case of Fig. 4.4-4 (ii) , difference pattern is observed with a lower gain than Fig. 4.4-4 (i). The lack of symmetricity of the difference pattern occurs due to the unequal power division to the patches. Fig. 4.4-4 (iii) shows maximum peak angle at $\theta < 0^0$ almost opposite compared to Fig. 4.4-4 (i).

Table 4.4-1 shows the performance summary of the proposed antenna between simulation and measurement. In the table, the performances of the proposed antenna are compared with the previously published pattern switchable antenna including the frequency, no of ports, gain, etc. The proposed antenna provides reasonable performance with simple compact geometry.

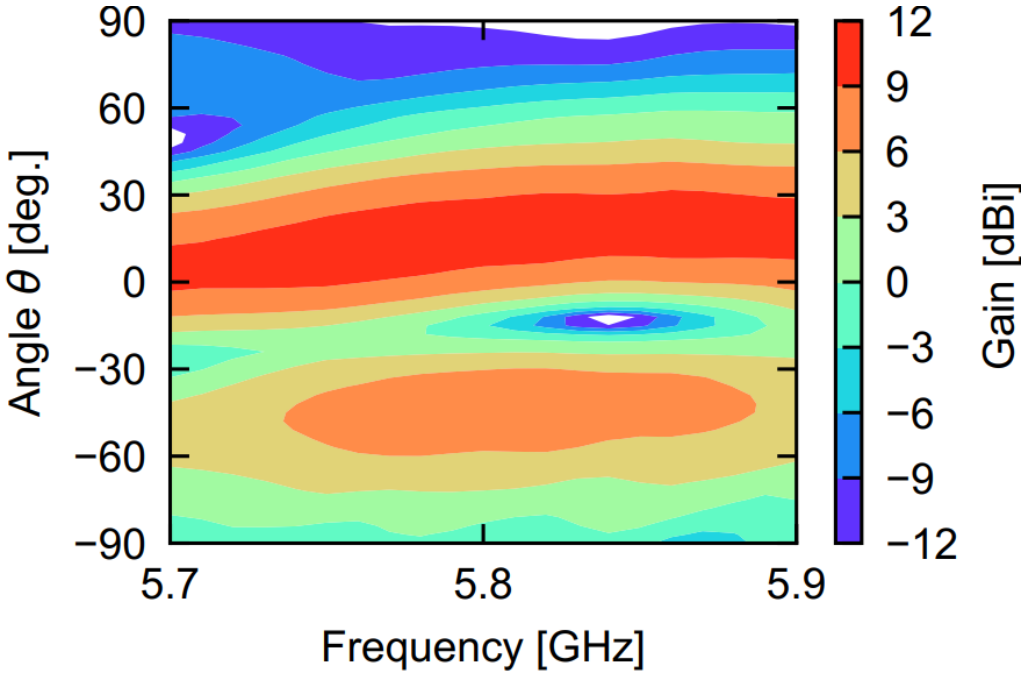

(i) State 1

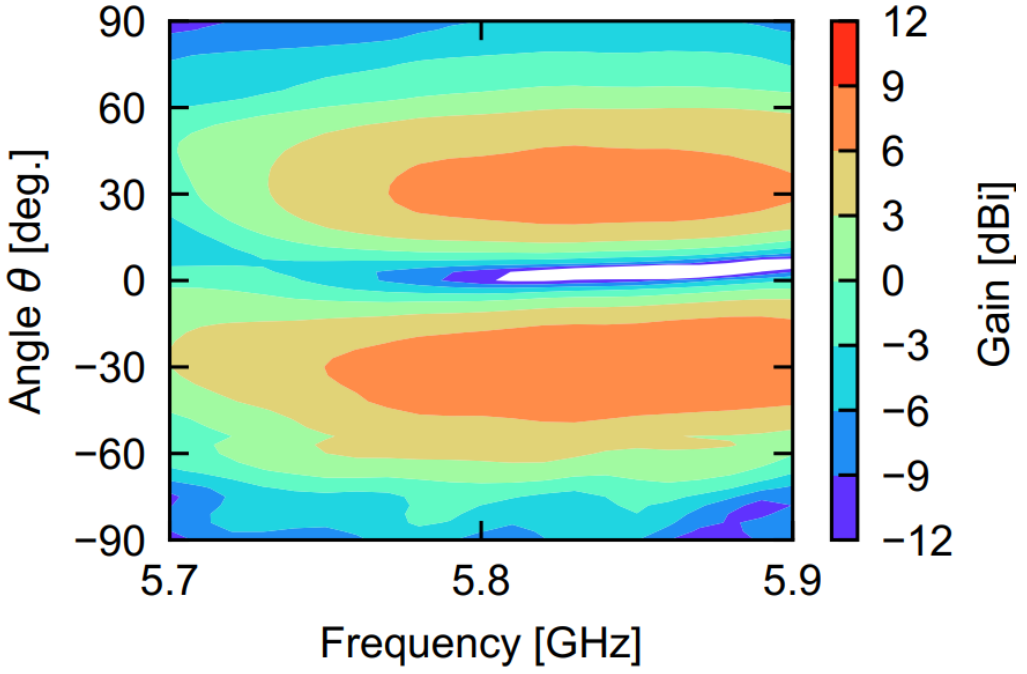

(ii) State 2

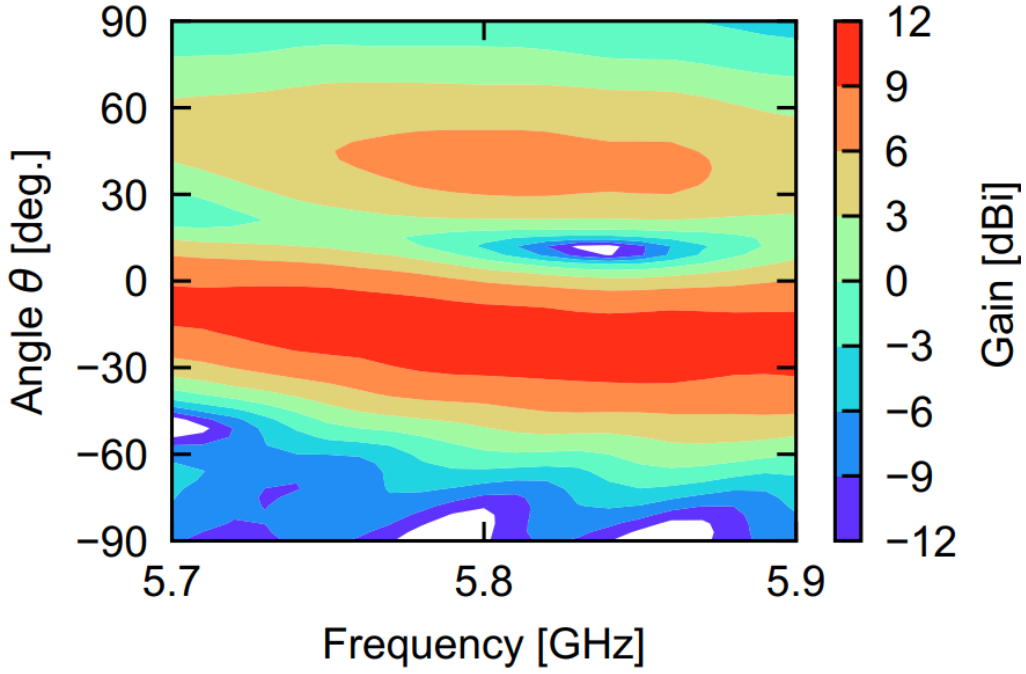

(iii) State 3

Figure 4.4-4: Measured radiation pattern versus frequency of the fabricated prototype antenna (i) State 1, (ii) State 2, (iii) State 3.

Table 4.4-1: Comparison of the proposed antenna with previously reported antennas.

Ref.	[3]	[36]	[1]	[37]	[34]	[31]	**Proposed**
Freq. [GHz]	5.8	5.8	5.8	2.4	2.4	5.8	**5.8**
No. of ant. Elements	2	4	2	1	4	4	**4**
Imp. BW. [GHz]	0.20	0.90	0.20	0.15	0.015	1.30	**0.26**
No. of Ports	4	4	1	1	2	2	**1**
No. of beams	4	4	2	4	2	2	**3**
Gain [dBi]	9.2	9.9	8.9	5.32	1	10.7	**10.5**

Chapter 5: CONCLUSION AND FUTURE WORKS.

Two different design of beam-steering antenna are discussed here. For first case, a single-feed dual-beam switchable characteristic of a novel antenna is presented in this paper. Three antenna elements with two active patches at a time are incorporated into PIN diodes to produce the beam switching. The prototype, which can tilt its broadside beam direction to $\pm 12°$ is built and fabricated.

For second case, a single-feed multi-beam switchable prototype array antenna is proposed. Four square patch antennas, four PIN diodes creating two SPDT switches, and two 90^0 hybrid couplers are responsible for the tilting of the main beam. The prototype can tilt its broadside direction to $\pm 14°$ and a third 33^0 sum beam and is fabricated and measured. The proposed theory is not limited to only 5.8-GHz application and can be applied to a broad range of frequencies keeping its simple design intact. Moreover, these antennas provide a low cost and reasonable gain with a single feed structure.

Bibliography

[1] N. Akther, M. Hasan, M. A. Hossain, E. Nishiyama, and I. Toyoda, "Experimental Study of Single-Feed Dual-Beam Switchable Array Antenna Using PIN Diodes for 5.8-GHz Application," in *2022 International Conference on Recent Progresses in Science, Engineering and Technology (ICRPSET)*, IEEE, 2022, pp. 1–4.

[2] L. Wai Leong *et al.*, "Beam Switching Antenna Modeling carbon nanotubes with different structure at millimeter wavelength antennas View project effect of electromagnetic field GSM-like at frequency 1800 MHz on rats female reproductive system physiology View project Beam Switching Antenna", doi: 10.13140/2.1.2739.8404.

[3] M. Hasan, E. Nishiyama, and I. Toyoda, "A Multi-Beam Array Antenna Employing Simple 4× 2 Beam-Forming Network Integrating Magic-T and Hybrid Coupler," in *2022 International Symposium on Antennas and Propagation (ISAP)*, IEEE, 2022, pp. 437–438.

[4] S. Y. Nusenu and E. Asare, "Butler Matrix Frequency Diverse Retrodirective Array Beamforming: An Energy-Efficient Technique for mmWave Networks," *Wirel Commun Mob Comput*, vol. 2020, 2020, doi: 10.1155/2020/9408519.

[5] N. C. Liu, C. C. Tien, C. Y. Chang, H. W. Ling, C. W. Chiu, and J. H. Tarng, "Millimeter-Wave 2-D Beam-Switchable and Scalable Phased Antenna Array," *IEEE Trans Antennas Propag*, vol. 69, no. 12, pp. 8997–9002, Dec. 2021, doi: 10.1109/TAP.2021.3098583.

[6] H. Zahra, M. Hussain, S. I. Naqvi, S. M. Abbas, and S. Mukhopadhyay, "A simple monopole antenna with a switchable beam for 5g millimeter-wave communication systems," *Electronics (Switzerland)*, vol. 10, no. 22, Nov. 2021, doi: 10.3390/electronics10222870.

[7] A. M. Mabrouk, A. A. Ibrahim, and H. F. A. Hamed, "Reconfigurable antenna with frequency and beam switching using transformer oil and PIN-diode for microwave applications," *Alexandria Engineering Journal*, vol. 61, no. 3, pp. 1824–1833, Mar. 2022, doi: 10.1016/j.aej.2021.06.099.

[8] C. Di Paola, S. Zhang, K. Zhao, Z. Ying, T. Bolin, and G. F. Pedersen, "Wideband Beam-Switchable 28 GHz Quasi-Yagi Array for Mobile Devices," *IEEE Trans Antennas Propag*, vol. 67, no. 11, pp. 6870–6882, Nov. 2019, doi: 10.1109/TAP.2019.2925189.

[9] H. Zhang, Y. Mahe, and T. Razban, "Low-cost Ku-band dual-polarized and beam switchable cross-type antenna array for satellite communications," *Microw Opt Technol Lett*, vol. 56, no. 11, pp. 2656–2659, 2014, doi: 10.1002/mop.28670.

[10] G. Mishra and S. K. Sharma, "A multifunctional full-polarization reconfigurable 28 ghz staggered butterfly 1-d-beam steering antenna," *IEEE Trans Antennas Propag*, vol. 69, no. 10, pp. 6468–6479, Oct. 2021, doi: 10.1109/TAP.2021.3070226.

[11] A. H. Murshed, M. A. Hossain, E. Nishiyama, and I. Toyoda, "Design and characterization of frequency reconfigurable honey bee antenna for cognitive radio application," *International Journal of Electrical and Computer*

Engineering, vol. 12, no. 6, pp. 6178–6186, Dec. 2022, doi: 10.11591/ijece.v12i6.pp6178-6186.

[12] M. V. Kuznetcov, S. K. Podilchak, A. J. McDermott, and M. Sellathurai, "Dual-Polarized High-Isolation Antenna Design and Beam Steering Array Enabling Full-Duplex Communications for Operation over a Wide Frequency Range," *IEEE Open Journal of Antennas and Propagation*, vol. 2, pp. 521–532, 2021, doi: 10.1109/OJAP.2021.3067471.

[13] N. M. Jizat, N. Ahmad, Z. Yusoff, N. M. Nor, and M. I. Sabran, "5G beam-steering 2x2 butler matrix with slotted waveguide antenna array," *Telkomnika (Telecommunication Computing Electronics and Control)*, vol. 17, no. 4, pp. 1656–1662, Aug. 2019, doi: 10.12928/TELKOMNIKA.V17I4.12777.

[14] I. Uchendu and J. Kelly, "Survey of Beam Steering Techniques Available for Millimeter Wave Applications," 2016.

[15] Z. Mousavi and P. Rezaei, "Millimetre-wave beam-steering array antenna by emphasising on improvement of Butler matrix features," *IET Microwaves, Antennas and Propagation*, vol. 13, no. 9, pp. 1287–1292, Jul. 2019, doi: 10.1049/iet-map.2018.5340.

[16] V. P. Kodgirwar, S. B. Deosarkar, and K. R. Joshi, "Design of Beam Steering-Switching Array for 5G S-Band Adaptive Antenna Applications–Part-I and Part-II," *IETE J Res*, vol. 68, no. 4, pp. 2909–2921, 2022, doi: 10.1080/03772063.2020.1732843.

[17] M. Hasan, E. Nishiyama, T. Tanaka, and I. Toyoda, "A first-harmonic push–push oscillator based active integrated dual-beam switchable array antenna," *Electron Lett*, vol. 59, no. 5, Mar. 2023, doi: 10.1049/ell2.12750.

[18] F. Ahmed, K. Singh, and K. P. Esselle, "State-of-the-Art Passive Beam-Steering Antenna Technologies: Challenges and Capabilities," *IEEE Access*, 2023, doi: 10.1109/ACCESS.2023.3278570.

[19] N. O. Parchin, H. J. Basherlou, Y. I. A. Al-Yasir, A. M. Abdulkhaleq, and R. A. Abd-Alhameed, "Reconfigurable antennas: Switching techniques— a survey," *Electronics (Switzerland)*, vol. 9, no. 2. MDPI AG, Feb. 01, 2020. doi: 10.3390/electronics9020336.

[20] C. Gu *et al.*, "Frequency-Agile Beam-Switchable Antenna," *IEEE Trans Antennas Propag*, vol. 65, no. 8, pp. 3819–3826, Aug. 2017, doi: 10.1109/TAP.2017.2713978.

[21] Z. M. Razi and P. Rezaei, "A two-layer beam-steering array antenna with 4 × 4 modified Butler matrix fed network for switched beam application," *International Journal of RF and Microwave Computer-Aided Engineering*, vol. 30, no. 2, Feb. 2020, doi: 10.1002/mmce.22028.

[22] S. A. Babale, O. Elijah, S. K. A. Rahim, and S. I. Orakwue, "Two-dimensional beam-steering phased-array utilizing 2× 2 Butler matrix," in *2017 IEEE 3rd International Conference on Electro-Technology for National Development (NIGERCON)*, IEEE, 2017, pp. 245–248.

[23] A. Pal, A. Mehta, D. Mirshekar-Syahkal, and H. Nakano, "A twelve-beam steering low-profile patch antenna with shorting vias for vehicular applications," *IEEE Trans Antennas Propag*, vol. 65, no. 8, pp. 3905–3912, 2017.

[24] J. Hu and Z.-C. Hao, "A two-dimensional beam-switchable patch array antenna with polarization-diversity for 5G applications," in *2018 IEEE MTT-S International Wireless Symposium (IWS)*, IEEE, 2018, pp. 1–3.

[25] Y. Geng, J. Wang, Y. Li, Z. Li, M. Chen, and Z. Zhang, "Radiation Pattern-Reconfigurable Leaky-Wave Antenna for Fixed-Frequency Beam Steering Based

on Substrate-Integrated Waveguide," *IEEE Antennas Wirel Propag Lett*, vol. 18, no. 2, pp. 387–391, Feb. 2019, doi: 10.1109/LAWP.2019.2892057.

[26] J. M. Wen, C. Yu, Y. X. Li, Y. M. Pan, and S. Y. Zheng, "A Compact Dual-Beam Steering Antenna Array Based on a Simplified Beamforming Network," *IEEE Trans Antennas Propag*, pp. 1–1, Jun. 2023, doi: 10.1109/tap.2023.3287402.

[27] Z. Qu, Y. Zhou, S. Alkaraki, J. R. Kelly, and Y. Gao, "Continuous Beam Steering Realized by Tunable Ground in a Patch Antenna," *IEEE Access*, vol. 11, pp. 4095–4104, 2023, doi: 10.1109/ACCESS.2023.3235597.

[28] T. Liang, Y. Pan, and Y. Dong, "Miniaturized Pattern-Reconfigurable Multimode Antennas with Continuous Beam-Steering Capability," *IEEE Trans Antennas Propag*, vol. 71, no. 6, pp. 4704–4713, Jun. 2023, doi: 10.1109/TAP.2023.3262146.

[29] I. Mujahidin, S. H. Pramono, and A. Muslim, "5.5 Ghz Directional Antenna with 90 Degree Phase Difference Output," in *2018 Electrical Power, Electronics, Communications, Controls and Informatics Seminar (EECCIS)*, IEEE, 2018, pp. 224–228.

[30] S. Shelar and N. Kolhare, "Design And Analysis of Hybrid Coupler," *vol*, vol. 3, pp. 1217–1220.

[31] T. Paing Phyoe, E. Nishiyama, and I. Toyoda, "A Magic-T Integrated 5.8-GHz Repeater Array Antenna Using Dual-Feed Network," 2019.

[32] Z. Duan, L. Xu, and W. Geyi, "Metal frame repeater antenna with partial slotted ground for bandwidth enhancement of wristband devices," *IET Microwaves, Antennas & Propagation*, vol. 11, no. 10, pp. 1438–1444, 2017.

[33] Y. Lee, J. Ha, and J. Choi, "Design of a wideband indoor repeater antenna with high isolation for 3G systems," *IEEE Antennas Wirel Propag Lett*, vol. 9, pp. 697–700, 2010.

[34] Y. J. Song and K. Sarabandi, "Miniaturized radio repeater for enhanced wireless connectivity of ad-hoc networks," *IEEE Trans Antennas Propag*, vol. 60, no. 8, pp. 3913–3920, 2012, doi: 10.1109/TAP.2012.2201124.

[35] Y. Lee, J. Ha, and J. Choi, "Design of an indoor repeater antenna with high isolation using metamaterials," *Microw Opt Technol Lett*, vol. 54, no. 3, pp. 755–761, Mar. 2012, doi: 10.1002/mop.26651.

[36] Y. Umeda, E. Nishiyama, and I. Toyoda, "A Beam-Forming Antenna Integrating Magic-T Based Matrix Feed Network," in *2022 International Symposium on Antennas and Propagation, ISAP 2022*, Institute of Electrical and Electronics Engineers Inc., 2022, pp. 433–434. doi: 10.1109/ISAP53582.2022.9998705.

[37] M. S. Alam and A. M. Abbosh, "Beam-Steerable Planar Antenna Using Circular Disc and Four PIN-Controlled Tapered Stubs for WiMAX and WLAN Applications," *IEEE Antennas Wirel Propag Lett*, vol. 15, pp. 980–983, 2016, doi: 10.1109/LAWP.2015.2489684.